BL-15C /2011G032

Background Correction to Experimental CCD Images of X-ray Diffraction, Showing a Temporal Oscillation of Pendellösung Interference Fringes

Jun-ichi Yoshimura and Keiichi Hirano
Photon Factory, Tsukuba 305-0801, Japan

In connection with the study of a strange temporal oscillation of X-ray Pendellösung interference fringes, conducted in the precision X-ray optics station BL-15C at PF-KEK, development of the way of background correction to raw X-ray images taken by a fiber-coupling CCD camera is described, along with a demonstration of how the quality of images and the reliability of data analysis are improved. As an additional subject, some special conditions or properties of diffraction images in this study are also explained.

1 Introduction

In these years since 2009, we have reported experimental observations of a strange temporal oscillation of X-ray Pendellösung interference fringes [1-3]. The observation has been made as synchrotron radiation diffraction experiment using X-ray CCD camera. Diffraction topographs of a silicon wedge crystal showing Pendellösung fringes were successively recorded onto the CCD camera, and an oscillation of fringes with elapsed time has been observed among the successively recorded images. The earliest observation was made using a type X-FDI 40mm camera (Photonic Science Ltd., pixel size 24.0 μm) [1-3]. Due to the author's (J.Y.) inexperience in using such CCD camera, acquired images were not received any after-processing such as dark field subtraction (hereafter DF subtraction), background correction (BG correction), and distortion correction (DT correction). The first reports above were made with such unprocessed images. Though thus imperfect data were used, correctness of the reports then should not heavily been damaged.

Since 2010, type X-FDI 11mm camera (pixel size 6.45 μm) has been used together with the X-FDI 40 mm type, to enable a higher resolution observation in space and time [4]. Also, results of the study have been reported with DF-subtracted image data since this year [5]. DT correction would not be necessary for X-FDI 11 mm camera since it is of non-tapered 1:1 transmission type [6]. However, images by X-FDI 40 mm camera seem to need DT-correction in our experience as well, if the images in the entire field are desired to be accurately analyzed.

In the early years of the study the importance of BG correction had not well been understood by the author (J.Y.). Nevertheless, its need gradually came to be known in the course of discussing analysis results of data images. In 2011, the way of BG correction for this study was developed spending a few months, and so far acquired data images were BG-corrected by this method. Since the presentation in 2012 [7], results of the study all have been reported with BG-corrected images . This report describes our experiences of BG correction, i.e. its way and the effect on the image quality and data analysis reliability.

2 Experimental Setup

We firstly explain the experimental setup (Fig. 1) of this study, though it has been shown in previous reports. The wavelength of the beam was chosen to be 0.081 nm (15.3 keV). Synchrotron beam from the double crystal monochromator (DCM, Si 111) was further monochromated and collimated by the collimator crystals (C1, C2; Si 220) (asymmetric factor was b≅0.1 both in C1 and C2). The angular width of the beam is reduced to 1/100 times there, and the spatial width is expanded to 100 times in the beam direction [8]. Thus, the wavelength spread of the incident beam onto the specimen becomes $\Delta\lambda_o/\lambda = 4.3 \times 10^{-4}$, and its angular width 0.034" for one wavelength, and 0.079" in the entire wavelength spread. The specimen (S) was a wedge crystal of silicon (FZ growth) as sketched in detail in the lower part of the figure. The 220 reflection was used in symmetric Laue geometry, the specimen being set in parallel setting with the upstream collimator crystals C2 and C1.The Bragg angle (θ_B) was then 12.2°. The spacing of Pendellösung fringes is calculated to be 0.345 mm. The angular width of diffraction power (Darwin width) of the specimen crystal is 2.50" against that of the incident beam 0.079".

Diffracted images from the specimen were recorded using an X-ray CCD camera (X-FDI 11mm, X-FDI 40 mm) as mentioned earlier, operated in non-fusion 12 bit mode and with gain = 1. Twenty, Forty, or more images were successively recorded with exposure time 0.2"–4.8" and with binning 1×1, 1× 2, 2× 2, ----, 4× 4, etc. The

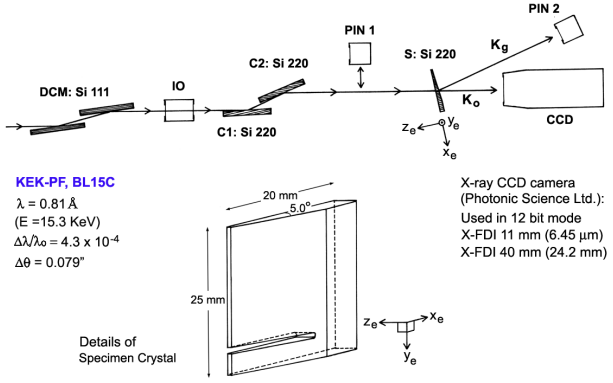

Fig. 1 Experimental setup of this synchrotron radiation study. For explanation of the figure, see text. x_e axis || [110], y_e axis || [-110], z_e axis || [001].

imaging was mainly made with the deviation angle (offset angle) of the specimen crystal set at zero, $\Delta\theta = 0$, but some image data were taken at off-peak angles $\Delta\theta = \pm 0.1" - \pm 0.3"$.

It should be added here that, while the angular adjustment of the specimen crystal was made with the intensity of diffracted image (G image, $\mathbf{K}_g$), recording of the specimen image was made for transmitted (or forward-diffracted) image (O image, $\mathbf{K}_o$). Rocking curve with respect to rotation of the crystal ($\Delta\theta$) is greatly different between O and G images. Usual X-ray topographs are of G image. Recording the O image nevertheless was not for some purpose, but a matter-of-course choice of setting the CCD camera in the horizontal position.

3 Background Correction

3.1 Its Need The necessity of back-ground correction came to be understood, by knowing the connection between a deep dip in the intensity profile of fringes and also unusually deep minimum in the amplitude distribution plot of fringe oscillation. Examples of deep dip in intensity profiles are shown in Fig. 2. The occurring sites of these intensity dips do not change among successively recorded data images. If such a deep intensity dip sits on a bottom in fringe profiles, position of the bottom is fixed there in the analyzing procedure and the fringe oscillation there is misleadingly concluded to be almost zero. Furthermore, it was known that similar intensity dips occur at the same sites in the image of collimator crystal (hereafter called blank image). From this fact, intensity dips were once considered to occur from some irregularities or distortions on the collimator crystal. However, afterward, they were known to be fixed in the CCD camera, from the fact that they occur always at the same sites in the image even when the collimator crystal was displaced. The author (J.Y.) finally came to understand the meaning of BG correction written in the user manual of the camera. Namely, the BG correction is a correction to the sensitivity non-uniformity (referred to as responsivity variations, in the user manual) peculiar to fiber-coupling CCD camera. While attention has been paid to intensity dips, intensity projection or protuberance also occurs from this sensitivity non-uniformity. Somewhat unusually high peak in fringe profiles would be caused by it. Such sensitivity non-uniformity can be overviewed in the top two profiles in Fig. 2. Fluctuation of the intensity there is roughly estimated to be ± 15 % of the mean intensity (see Fig. 4, more exactly). This is a large error not to be neglected. Need of developing a way of the proper BG correction was realized, although intensity dips had been corrected by a *fill-in-pits* computer program until then. The work for the BG correction was done in 2011, as described earlier.

3.2 Practice of the Correction For BG correction, a reference image is necessary to do it. In the case of this study, use of the image from the collimator crystal is soon thought of. Though at first it was concerned whether the collimator image was good for the purpose as the

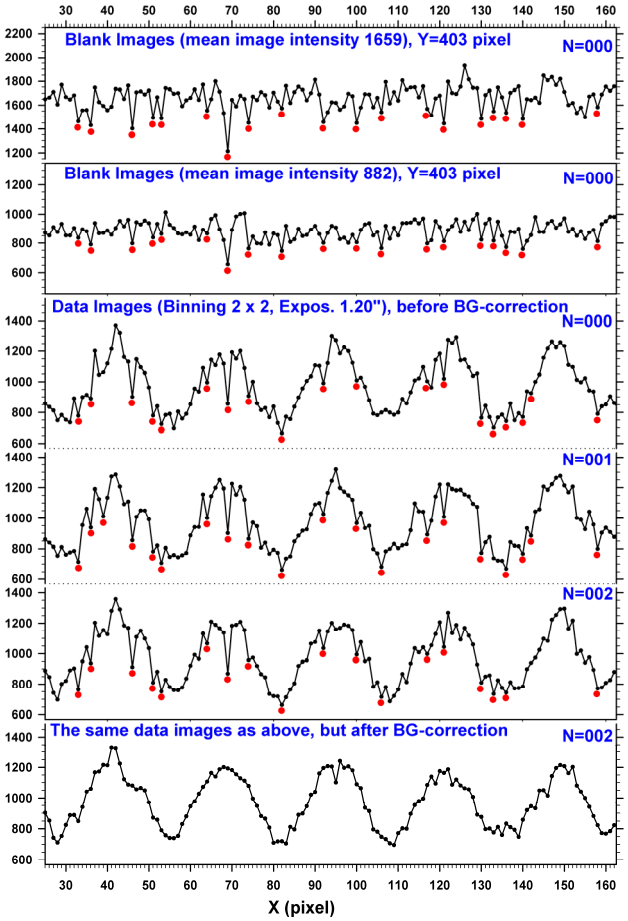

Fig. 2 Intensity profiles scanned along the X-axis in the images of the collimator (top two) and the specimen crystal before BG correction (except for the lowest one). Red circles mark deep intensity dips discussed in the text. The images were taken by X-FDI 11mm camera with binning 2 × 2. The scanning was made at Y=403 pixel with one pixel width for all the profiles.

reference image, the result was successful than had been considered. From the start of this study before considering BG correction, diffraction images from the collimator crystal(C2) had been recorded in machine-time experiments as reference for general purposes, under the same conditions with the specimen images (binning, exposure time, successive recording of twenty image), and at several intensities. The intensity of recorded collimator images was adjusted by placing an appropriate absorber (plates of quartz, aluminum; X-ray films) just in front of the camera window.

A stack file of the collimator image (hereafter, *blank image*) of the mean image intensity near that of a specimen image (hereafter, *subject image*) receiving BG correction, was broken to twenty individual images. The broken images were added up to an integrated image using *Process>Image Calculator>Add* command of *ImageJ*. The integrated image was divided by 20 using *Process>Math>Divide* command, to give the mean intensity image (*blank-mean.tif*). Its mean intensity (*mean int.*) was obtained with respect to the entire field of the *blank–mean.tif* image. Further, this image was converted

from 16 bit type to 32 bit type, using *Image>Type* command. (Images were of 12 bit type when recorded by the CCD camera, but afterward converted to 16 bit type so that they can be handled in *ImageJ*.) The 32 bit-converted *blank-mean.tif* image was divided by the *mean int*. intensity, using *Math >Divide* command. Thus, the reference image (*blank-mean7.tif*) was prepared, where the image intensity is given to 7-th or 8-th decimal place with the mean intensity one. The 32 bit conversion was necessary to give intensity values of significant (usable) precision to the normalized mean intensity image. The subject images as stacked in one file was divided pixel by pixel by this *blank–mean7.tif* image, using *Process>Image Calculator>Divide* command. Thus, the stack file of BG corrected subject images (*subject-Bcorr.tif*) was made up.

Fig. 3 shows an example of *blank–mean.tif* image of binning 2×2. (Binning was written like BN:1×1, BN:2×2, hereafter. White contrast indicates higher intensity in the image.) The entire field as received by the CCD camera is shown. Fig. 4 shows intensity profiles scanned on *blank –mean.tif* images (BN:1×1, BN:2×2). The Y=296 profile of the BN:2×2 image is concerned with a subject image profile shown later in Fig. 7. The protuberance seen in X=400-450 in this profile is not a real intensity variation in the blank image, but is due to a rapid increase in the camera sensitivity in the limited area. The scanned positions are indicated by arrows in Fig. 3. Sites where the sensitivity varies thus greatly are limited. As seen in the top profile in Fig.4, intensity dips in the BN:1×1 image is very deep. In the example shown, the intensity variation there is 991.4 (mean) ± 78.3 (std dev) in statistics, but the maximum and minimum intensities are, respectively, 991.4 + 173.6 and 991.4 – 357.4. The intensity variations in the BN:2×2 image (Y=282 pixel) is 1191.3 ± 66.4, and the maximum and minimum intensities are, respectively, 1191.3 +171.3 and 1191.3–309.3. So far as known by our some checks, the map of such sensitivity non-uniformity does not change in a short time, but seems to somewhat or non-negligibly vary in a time elapse of 1 or 2 years.

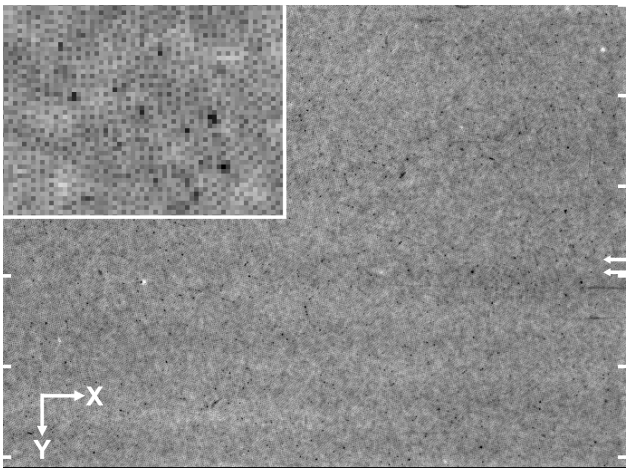

Fig. 3 Example of reference image (mean intensity 1160.3) used in BG correction. Binning 2×2. White tick marks graduate every 100 pixels (1.29 mm) from the top of the image. The inset is a magnification (×100) of a part of the matrix image.

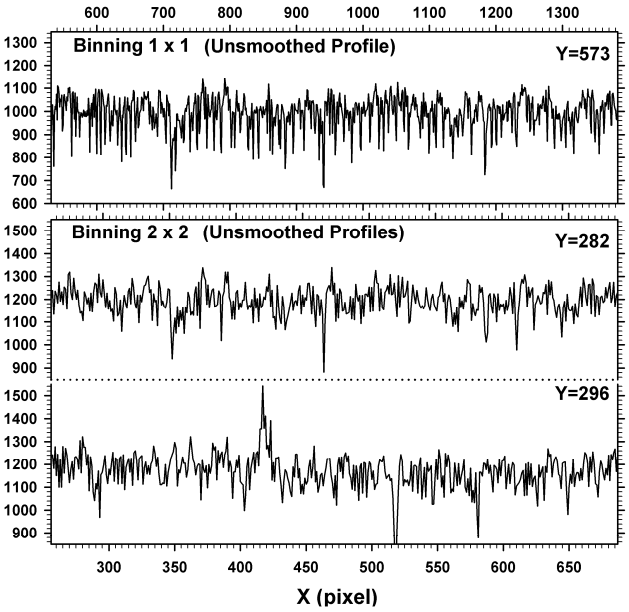

Fig. 4 Intensity profiles scanned on reference images of BN:1×1 (top) and BN:2×2 (bottom 2), to show the sensitivity variations in a CCD camera (X-FDI 11 mm).

3.3 Results Figs. 5 and 6 compare subject images before and after BG correction respectively with BN: 1×1 and BN:2×2 images. As is seen, the improvement of image quality in the BN:1×1 image is striking. The ground of the image became much smoother without noisy intensity disturbances, than before BG correction, and effective resolution of the image was much enhanced. Thin lines and small spots (point-like defect images) invisible before BG correction became well visible, and point-like defect images visible before BG correction show more exact appearance so that their fine structures appear precisely. Furthermore, fringe contrast was improved at least in impression by visual inspection, particularly in the low-contrast region. Image quality of the BN:2×2 image similarly was improved. The ground of the image is less smooth than that of the BN:1×1 image, probably because BG correction is less precise due to the binning structure 2×2. However, all the improvements noticed in the BN:1×1 image were similarly found inthe BN:2×2 image. Thin lines and small spots which became visible in the BN:1×1 image, similarly became visible in this image. Such improvements change our previous view to the CCD camera. Letter A-D in the presented images mark noticeable images of defects or the like. Comments to them are given in Sec. 4.

Through this developing work of BG correction, it was known that intensity variations on the diffracted image of the collimator, *i.e.* blank image, is much smaller and much more slowly varying than that due to the sensitivity non-uniformity of the CCD camera. During the machine time experiment over several days, it happens that position of the collimator image is somewhat displace for

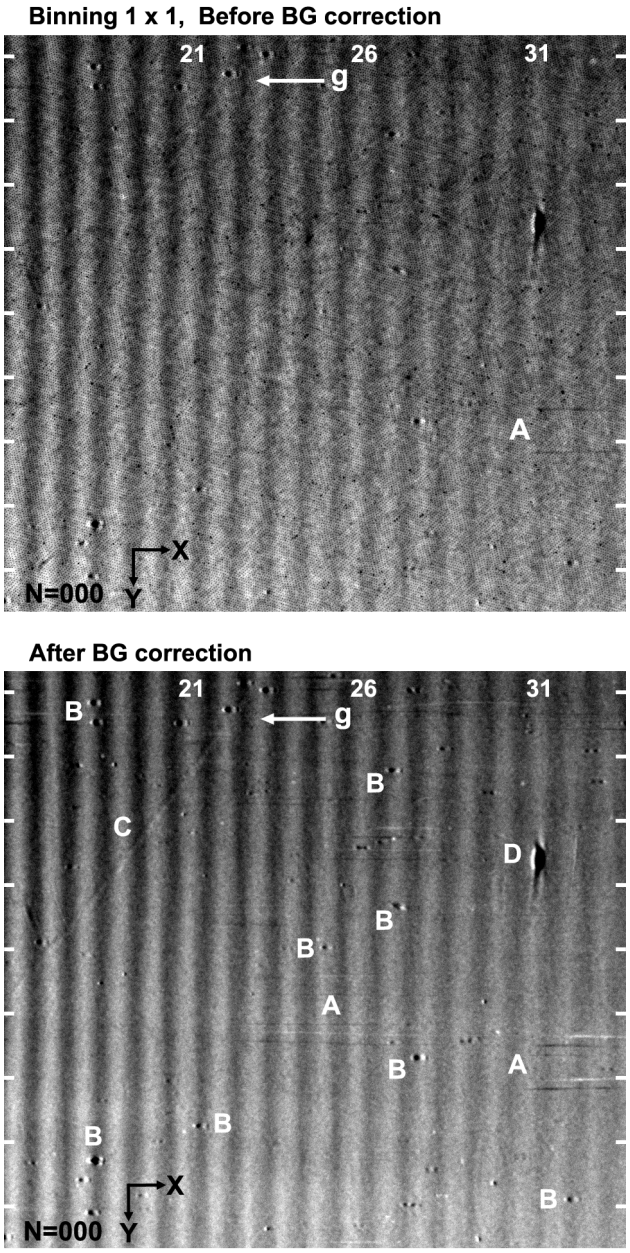

Fig. 5 Comparison of subject image with binning 1×1 before and after BG correction. Tick marks graduate every 100 pixels (0.645 mm) from the top of the image. Top numerals give the number.

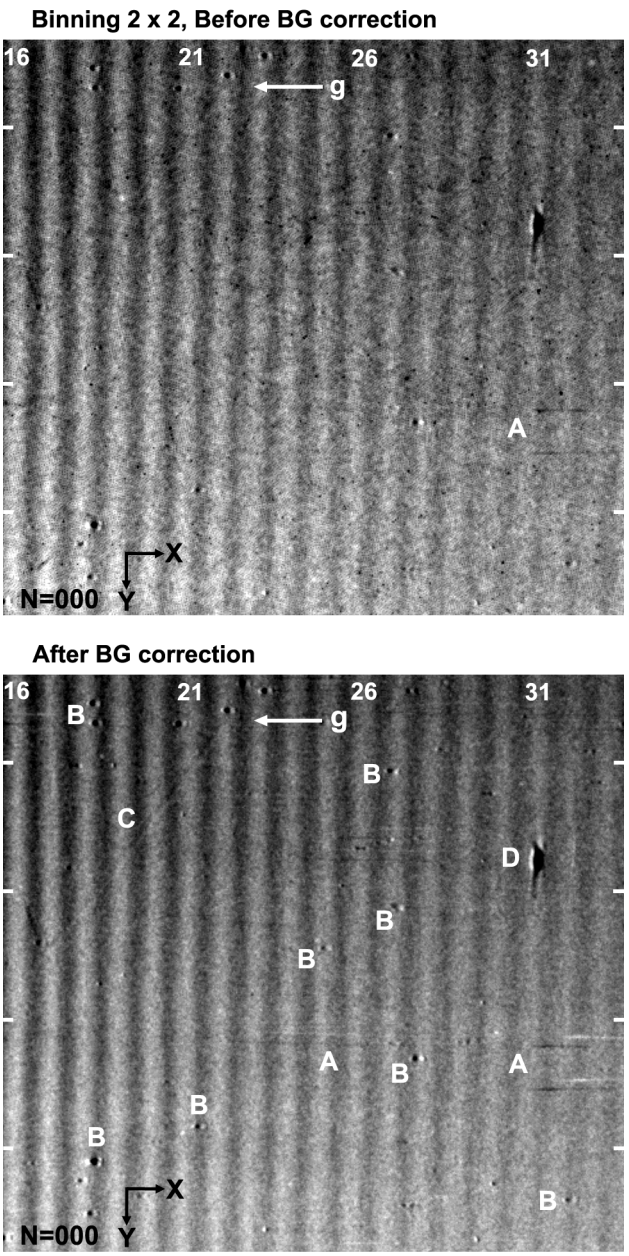

Fig. 6 Comparison of subject image with binning 2×2 before and after BG correction. Tick marks graduate every 100 pixels (1.29 mm) from the top of the image

some reasons, and its diffracted intensity somewhat varies due to small angular drift of concerned crystals. However, the influence of such changes is negligibly small on the present BG correction.

Figs. 7a and 7b compare intensity profiles before and after BG correction with respect to the BN:2×2 subject image. Difference between fringe profiles before and after BG correction is also remarkable. Deep or fairly deep intensity dips before BG correction at the sites X=517-518, X=546 and X=580, all disappear after BG correction. The high and broad fringe profile (Fr. No. 24) at X≅420 results from the local rapid increase in the camera sensitivity as mentioned with Fig. 4. Fig. 8 compares amplitude distribution plots of fringe oscillation before and after BG correction. The plots are a main result of analyzing fringe profiles. The oscillation amplitude here was obtained as $\sqrt{2}$ × [standard deviation of the fringe position oscillation in twenty successive recorded images]. Comparison is shown for the fringe oscillations measured in the top and in the bottom of profiles. Numerals attached to some of data points give a label number of the concerned fringes (see also Fig. 6, Fig. 7a and 7b). Oscillation amplitudes before BG correction vary violently with fringes both at the top and bottom of fringes, presumably because the disorder in fringe profiles is amplified, and made more complicated by the

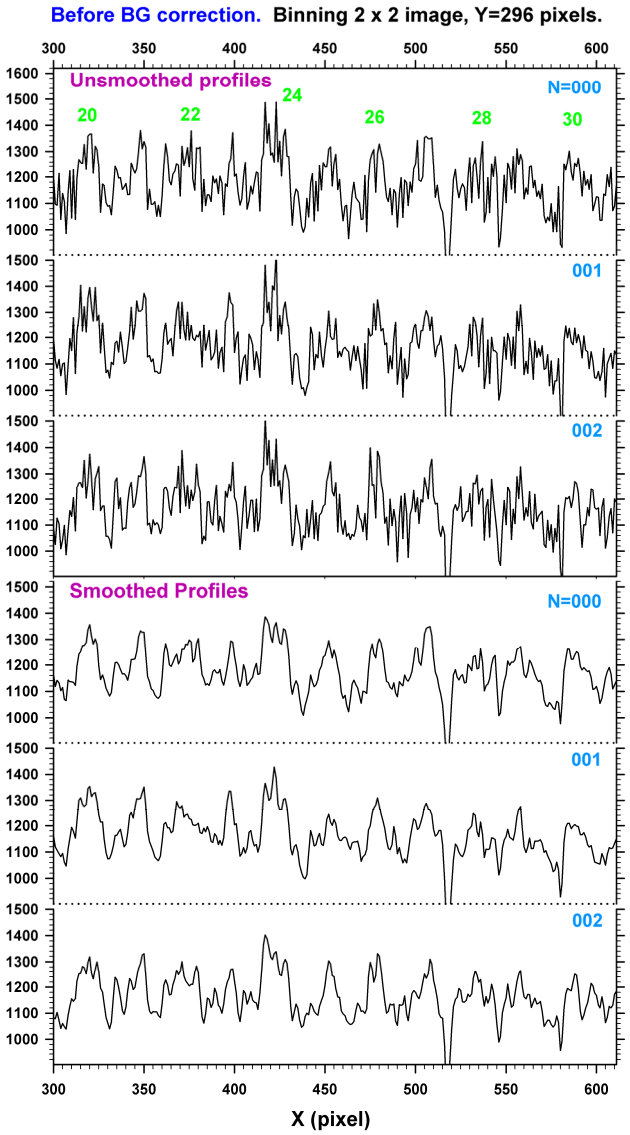

Fig. 7a Intensity profiles scanned on a subject image (BN:2×2) before BG correction. Scanned on the line Y=296 with one pixel width.

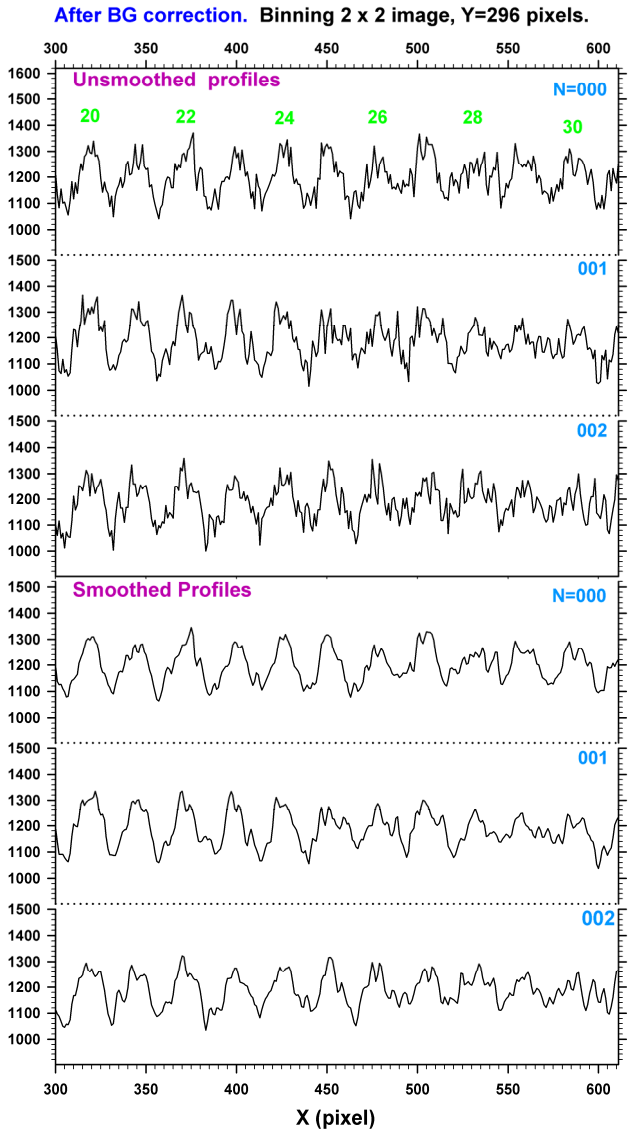

Fig. 7b Intensity profiles scanned on a subject image (BN:2×2) after BG correction. Scanned on the same position as Fig. 7a.

sensitivity non-uniformity. Deep amplitude dips marked with ( ) in the bottom-position amplitude plot would have been caused by the coincidence with deep sensitivity dips of the camera, which resulted in the seeming fixing of the bottom positions.

4 Further Comments on Subject Images

We firstly explain features marked with letters "A" – "D" in Figs. 5 and 6.

A: Thin, horizontal linear images, black and white, originate from a similar image in the blank image, which probably is caused by a scratch flaw on the collimator crystal. The black line is propagated to the subject image which receives the blank image as the incident image. The white line is a seal of the same black line in the blank image, which was registered in the subject image when it was divided by the reference image made from this blank image. The black and white line properly should be coincided. However, their actual positions are displaced each other by *ca* 0.1 mm in real dimension (about 8 pixels in the B:2×2 pixel size). This gap occurred because the position of the blank image was shifted by the mentioned length in the time elapse between the recordings of the blank and subject images. Similar sets of black and white lines of the same origin are seen also in other places in Figs. 5and 6. Though it is not yet enough clear, presence of such linear image (black line) seems to have influence on the fringe oscillation in the surrounding region.

B: These are images of point-like defects (precipitates) in the specimen crystal. Other unmarked spot images also are of the same origin. By the BG correction, spot images up to very small ones were made visible. Although the specimen should be a highly perfect as-grown crystal of FZ growth, not a small number of point-like defects are thus revealed. This would be in large measure due to high strain-sensitivity of the topographic method, as well as to high resolution of the image. From the beginning, data

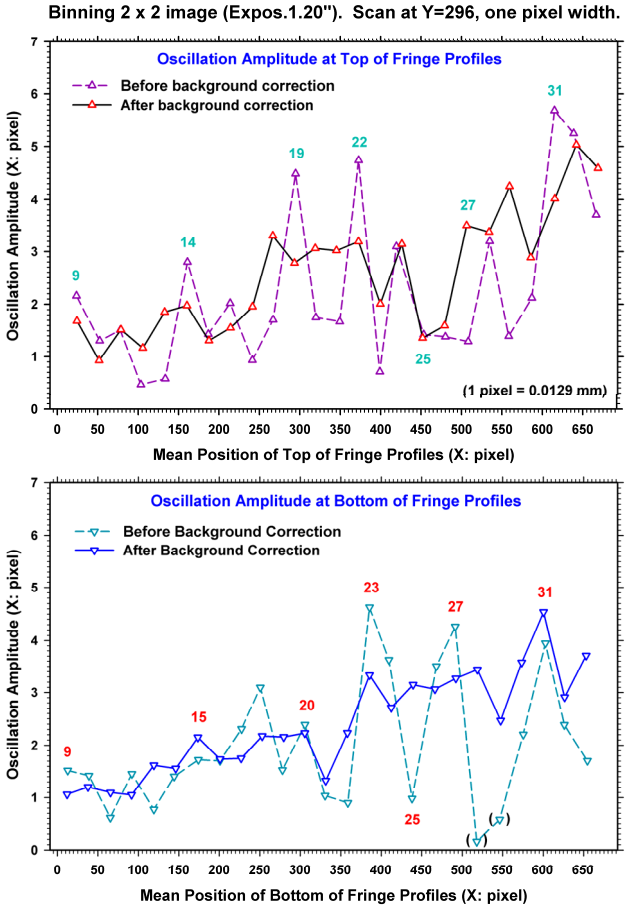

Fig. 8 Comparison of amplitude plots of temporal fringe oscillation before and after BG correction. These are the result of analyzing fringe profiles as illustrated in Figs. 7a and 7b. Numerals attached to data points are a label number of the respective fringes concerned.

images in this study (particularly subject images) may be referred to as a quasi-plane-wave topograph having high sensitivity to crystal distortion, and further made much more strain-sensitive by the fact that images were taken as the O image at $\Delta\theta = 0$ where the slope of rocking curve is most steep. Many defects and scratch flaws seen in the present subject images would not to be revealed by usual high sensitive topography.

Point-like defect images seem to influence the fringe oscillation, and really influence the profile analysis. However, their way to have influence is not well understandable. Defect images of strong contrast as marked with B do not change their position of the maximum or the minimum intensity, in the successive images. If such a spot image sits on the top or the bottom of fringes, the top or the bottom position is seemingly fixed there, and does not show oscillation in the fringe profile analysis. On the other hand small and/or weakly contrasted spot images change their appearance and intensity-extremum position in successive images. If such a spot image sits on the top or the bottom of fringes, they in many cases seem to amplify the fringe oscillation there. However, in some cases, fringe oscillation does not almost seem to be influenced by such spot images.

C: This rather diffuse linear image is the trace of scratch flaw which was introduced in polishing the crystal and remains not completely removed by etching. Residual strain with the scratch flaw would be very weak, but is revealed in the present high sensitivity topographs. Where such a linear image crosses the bottom of fringes, the fringe oscillation at the crossed position is amplified in many cases.

D: This image is not of a defect in the specimen crystal, but is connected with an origin in the blank image. It migrates on the subject image according to the change in the position of the collimator crystal (C2) relative to the specimen. The responsible site is located in the blank image. However, only a thin, short linear image of weak contrast is seen there. It is unknown why such a linear image causes a large spot image in the specimen crystal.

Finally, it should be known that the effective deviation angle of diffraction $\Delta\theta_{eff}$ varies along the Y direction in the subject images. This is not an experimental error, but is a normal property of multi-crystal non-parallel (+, −) setting topography (see Fig. 1), in accordance with the effect of vertical divergence of the beam [9]. Though it is not ready to give a quantitative estimation, $\Delta\theta_{eff}$ qualitatively increases from bottom to top in the images. From the variation in the fringe spacing, the deviation angle becomes $\Delta\theta_{eff} = 0$ near the top of the images. According to dynamical diffraction theory, all the characteristics of the image are governed by $\Delta\theta_{eff}$. The decrease in the image intensity from bottom to top is the case, and corresponds to the rapid decrease in the diffracted intensity from low to high angle side on the rocking curve of the O beam. In such field we study the oscillation of Pendellösung fringes, and strive to find any law there.

References

[1] J. Yoshimura and K. Hirano, *22-th Annual Meeting of Japanese Society for Synchrotron Radiation Research*, Abstract p. 127 (2009) [in Japanese].

[2] J. Yoshimura and K. Hirano, *Meeting Abstract of the Physical Society of Japan*, Vol. 69, Issue 1, Pt.4, p. 946 (2009) [in Japanese].

[3] J. Yoshimura and K. Hirano, *J. Synchrotron Rad*. **16**, 601 (2009).

[4] J. Yoshimura and K. Hirano, *Meeting Abstract of the Physical Society of Japan*, Vol. 70, Issue 1, Pt.4, p. 967 (2010) [in Japanese].

[5] J. Yoshimura and K. Hirano, *Meeting Abstract of the Physical Society of Japan*, Vol. 70, Issue 2, Pt.4, p. 887 (2010) [in Japanese].

[6] S. Kishimoto and Y. Tanaka, *Detector Guide to Synchrotron Radiation Users* (Tokyo, 2011) [in Japanese].

[7] J. Yoshimura and K. Hirano, *25-th Annual Meeting of Japanese Society for Synchrotron Radiation Research*, Abstract p. 131 (2012) [in Japanese].

[8] S. Kikuta, *X-Ray Diffraction and Scattering,* Vol.1 (Tokyo, 1992) [in Japanese].

[9] J. Yoshimura, *J. Appl. Crystallogr*. **17**, 426 (1984).